Atmos. Meas. Tech. Discuss., https://doi.org/10.5194/amt-2019-90
Manuscript under review for journal Atmos. Meas. Tech.
Discussion started: 5 April 2019

Atmospheric Measurement Techniques Discussions

Intercomparison of aerosol volume size distributions derived from AERONET ground based remote sensing and LARGE in situ aircraft profiles during the 2011-2014 DRAGON and DISCOVER-AQ experiments

Joel S. Schafer[1], Tom F. Eck[2], Brent N. Holben[3], Kenneth L. Thornhill[4], Luke D. Ziemba[4], Patricia Sawamura[4], Ilya Slutsker[1], Bruce E. Anderson[4], Alexander Sinyuk[1], Dave Giles[1], Alexander Smirnov[1], Andreas J. Beyersdorf[4,5], and Edward L. Winstead[4]

[1]Science Systems and Applications, Inc. Lanham, MD, USA
[2]Universities Space Research Association, Columbia, MD, USA
[3]NASA Goddard Space Flight Center, Greenbelt, MD, USA
[4]NASA Langley Research Center, Hampton, Virginia, USA
[5]University of California at San Bernardino, CA, USA

Correspondence: Joel Schafer (joel.schafer@nasa.gov)

Abstract.

Aerosol volume size distributions (VSD) retrievals from the Aerosol Robotic Network (AERONET) aerosol monitoring network were obtained during multiple DRAGON (Distributed Regional Aerosol Gridded Observational Network) conducted in Maryland, California, Texas and Colorado from 2011 to 2014 . These VSD products were used during field campaigns to make comparisons with near simultaneous in situ sampling from aircraft profiles carried out by the NASA Langley Aerosol Group Experiment (LARGE) team as part of four campaigns comprising the DISCOVER-AQ (Deriving Information on Surface conditions from Column and Vertically Resolved Observations Relevant to Air Quality) experiments. For coincident ($\pm$ 1 hour) measurements there were a total of 91 profile-averaged fine mode size distributions acquired with the LARGE Ultra-High Sensitivity Aerosol Spectrometer (UHSAS) instrument matched to 153 AERONET size distributions retrieved from almucantars at 22 different ground sites. These volume size distributions were characterized by two fine mode parameters, radius of peak concentration (r_{peak_conc}) and VSD fine mode width ($width_{fine\_mode}$). The AERONET retrievals of these VSD fine mode parameters, derived from ground-based almucantar sun photometer data, represent ambient humidity values while the LARGE aircraft spiral profile retrievals provide dried aerosol (RH<20%) values. For the combined multiple campaign data set, the average difference in r_{peak_conc} was 0.033 $\pm$ 0.035 μm (ambient AERONET values were 15.8% larger than dried LARGE values) and the average difference in $width_{fine\_mode}$ was 0.042 $\pm$ 0.039 μm (AERONET values were 25.7% larger). When the LARGE retrieved values were adjusted to account for ambient humidification, the agreement notably improved with AERONET-LARGE average differences for r_{peak_conc} decreasing to 0.011 $\pm$ 0.019 μm (AERONET values 5.2% larger) and $width_{fine\_mode}$ average differences decreasing to 0.030 $\pm$ 0.037 μm (AERONET values 15.8% larger).

Atmos. Meas. Tech. Discuss., https://doi.org/10.5194/amt-2019-90
Manuscript under review for journal Atmos. Meas. Tech.
Discussion started: 5 April 2019

Atmospheric Measurement Techniques Discussions

1 Introduction

Atmospheric aerosol volume size distribution information is relevant to modeling of radiative transfer, weather processes and human health via air quality concerns [Peng et al. (2018), Li et al. (2015), Sheng et al. (2019), Eilenberg et al. (2018), Gong et al. (2003)]. Interactions of atmospheric aerosols with clouds are highly sensitive to their size distributions [Feingold (2003)]. Current climate models are now able to simulate the full aerosol size distributions and therefore benefit from accurate aerosol size parameterization [Li et al. (2015)]. Geographic and seasonal variability in atmospheric aerosol due to differences in aerosol type and composition were historically difficult to capture globally at high temporal resolutions. The Aerosol Robotic Network (AERONET) global monitoring program provides an opportunity to capture seasonal and diurnal trends in extinction-weighted column integrated aerosol volume size distribution and concentration derived from frequent sky radiance measurements and spectral aerosol optical depth.

Very few direct comparisons of size distribution between in situ and AERONET retrievals have been published. Eck et al. (2012) summarized a number of region-specific comparison studies focused on both fine and coarse mode. During INDOEX Clarke et al. (2002) computed lognormal fits of volume size distributions for in situ measurements for fine mode pollution acquired by ship and aircraft in the Arabian Sea under high aerosol loading and found average accumulation mode volume peak radius ranged from 0.17 to 0.18 μm with computed geometric standard deviations for ship data equal to 1.51 and aircraft data equal to 1.43. These values are similar to the AERONET retrieved averages from 1998 to 2000 in the Maldives (Kaashidhoo) in the same region. For this 2 year observation period the AERONET determined average volume median radius was 0.18 μm with a width of 1.49 for almucantars taken with AOD at 440nm exceeding 0.4 which agrees well with the Clarke et al. (2002) results. Reid et al. (2005) investigated the agreement of in situ measurements of the volume median radius for smoke from various distinct regions of biomass burning; Southern Africa, North America (temperate and boreal) and South America) with retrievals from AERONET. For each region, the in situ volume median diameter typically agreed with AERONET retrievals within $\sim$ 0.01 mm. Retrievals of larger radius (sub-micron) aerosol from AERONET almucantars have also compared well with in situ data as detailed in Eck et al. (2010) where Pinatubo stratospheric peak volume radius of $\sim$ 0.56 μm derived from AERONET retrievals was very similar to the effective radius of 0.53 μm noted by Pueschel et al. (1994) based on in situ stratospheric aircraft measurement.

This paper presents a large number of comparisons of multiple fine mode volume size distribution datasets from four US regions for in-situ measurements from repeated aircraft profiles during a series of month-long intensive DISCOVER-AQ campaigns conducted between 2011 and 2014. Given the typical complexity of aircraft campaigns and the fact that validation of AERONET retrieval products is rarely a central campaign goal, this well-coordinated effort resulted in a dataset unique for the quantity and near simultaneous nature of the comparisons.

2 Instrumentation

In the summer of 2011 AERONET deployed more than forty Cimel sun photometers in the Baltimore-Washington, DC region as part of DRAGON (Distributed Regional Aerosol Gridded Observational Network) campaign of which five were located

Atmos. Meas. Tech. Discuss., https://doi.org/10.5194/amt-2019-90
Manuscript under review for journal Atmos. Meas. Tech.
Discussion started: 5 April 2019

Atmospheric Measurement Techniques Discussions

at DISCOVER-AQ aircraft profile sites. The AERONET DRAGON mesoscale network was comprised of automatic sun/sky radiometers distributed on a roughly 10km grid (covering an area of approximately 60km x 120km; average distance between sites= 9.9km) which operated continuously for more than 2 months. Subsequent campaigns were less densely instrumented each using approximately 15 ground sites (5-6 of which were profile sites) in the San Joaquin Valley (California), Houston Metro (Texas) and Colorado Front Range with average distance between sites ranging from 20-25km. The DRAGON ground networks for each campaign are depicted in Figure 1; vertical spiral profile sites used are shown in red.

The AERONET DRAGON campaign was concurrent with the NASA sponsored DISCOVER-AQ air quality experiment which performed daily research flights concentrating on repeated multiple daily profile measurements of gaseous and particulate pollution over typically 5-6 primary sun photometer sites. The number of flights days for each campaign ranged from 10 to 16 with atmospheric conditions ranging from very low aerosol optical depth (AOD) with low column water vapor (AOD 500nm < 0.05; CWV < 1cm) to hazy and humid (AOD 500nm $\sim$ 0.81; CWV > 4.5cm).

A complete description of the sun photometers used is provided by Holben et al. (1998). All sun photometers at profile sites had narrow bandpass filters with central wavelengths of 340, 380, 440, 500, 675, 870, 940, 1020 and 1640nm which cover the visible and near infrared spectrum. Eck et al. (1999) describes the uncertainty in aerosol optical depth which varies with wavelength (larger in the ultraviolet) and ranges from $\sim$ 0.01-0.021 for sun photometers during deployment. Direct solar irradiance is measured at each wavelength (FOV 1.2°) as well as radiance from the sky in both the principal plane ($\sim$ 9 times daily) and the solar almucantar ($\sim$ 8 times daily) which is taken at four wavelengths (440, 675, 870 and 1020nm). The almucantar procedure records sky radiance every 0.5° close to the position of the sun (< 6°) and with decreasing angular frequency further from the sun (2°-10°). Both aerosol optical depth measurements and sky radiance from almucantars are input to inversion code used to routinely produce AERONET retrievals of volume size distribution, phase function, real and imaginary component of refractive index, effective radius and single scattering albedo [Dubovik and King (2000); Dubovik et al. (2002); Dubovik et al. (2006)]. The AERONET retrieval products have quality controls applied based on Holben et al. (2006). Both aerosol optical depth (AOD) and alumucantar retrievals are from the version 3 dataset (version 3 data released in January 2018) [Giles et al. (2019)].

In-situ aerosol properties were measured on the NASA P-3B aircraft by the NASA Langley Aerosol Group (LARGE) team using a suite of instruments to characterize ambient aerosol optical and microphysical properties [Beyersdorf et al. (2016)]. A DMT Ultra-High Sensitivity Aerosol Spectrometer (UHSAS) calibrated with ammonium sulfate was utilized for particle sizing measurements. Although the UHSAS instrument only covers most of the fine mode size range (radius: 0.05-0.5 μm), it does allow for an assessment of the agreement of peak volume radius, size distribution width over a moderately large range of AODs. Aerosol optical measurements were made with a pair of TSI-3563 3-wavelength integrating nephelometer (TSI, Inc. model 3563) and a 3-wavelength Radiance Research Particle Soot Absorption Photometer (PSAP, Radiance Research). The tandem nephelometers were run with and without humidification to find the dry scattering (approximately 20% relative humidity) and humidified scattering coefficients (approximately 80% relative humidity). Scattering at ambient relative humidity was then calculated based on a single-parameter monotonic growth factor – gamma [Gassó et al. (2000)]. Scattering coefficients at 450,

Atmos. Meas. Tech. Discuss., https://doi.org/10.5194/amt-2019-90
Manuscript under review for journal Atmos. Meas. Tech.
Discussion started: 5 April 2019

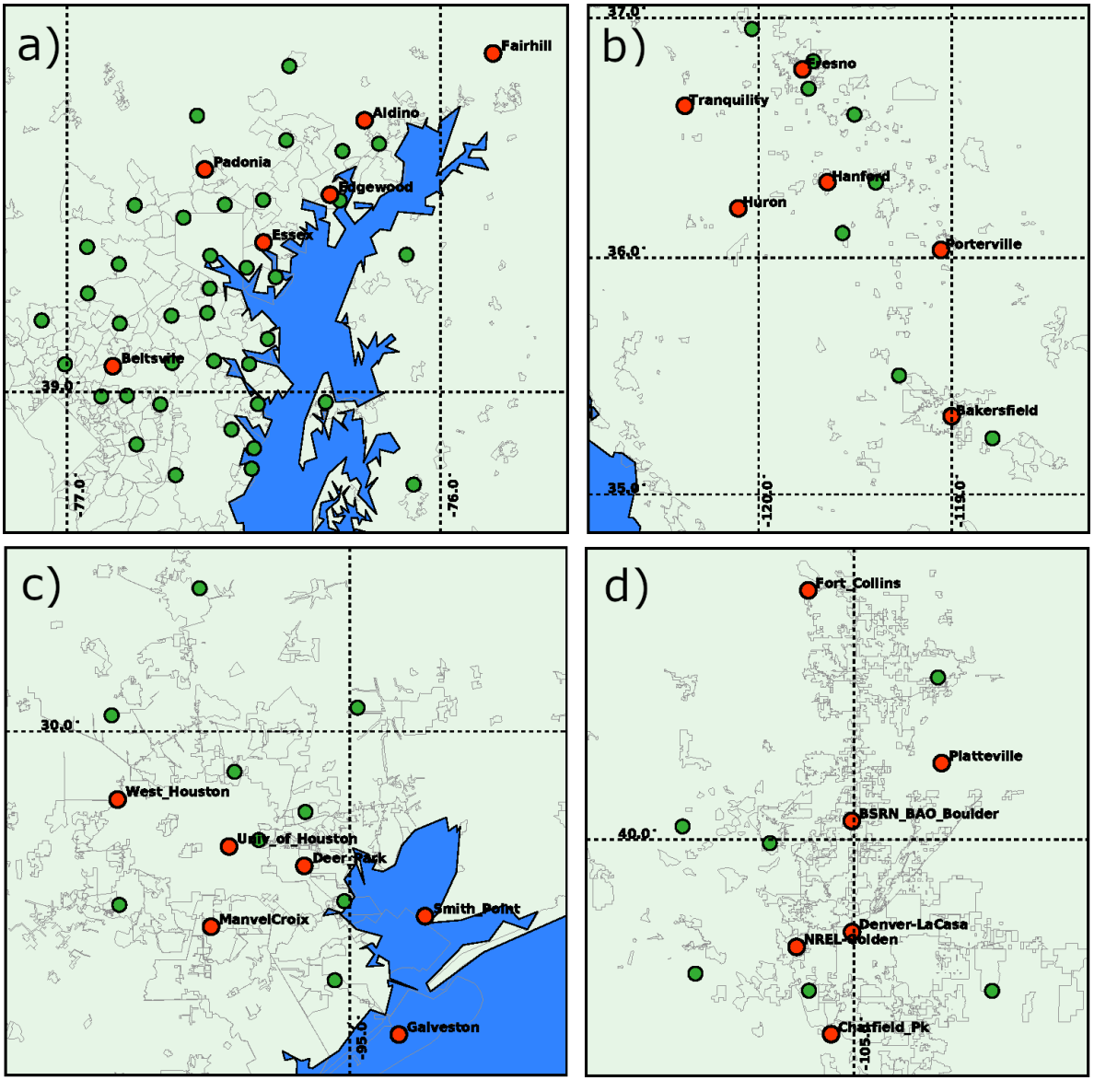

Figure 1. The AERONET ground networks are shown for each campaign. Profile sites used are shown in red with urban boundaries overlaid in gray. a) Maryland b) California c) Colorado d) Texas

Atmos. Meas. Tech. Discuss., https://doi.org/10.5194/amt-2019-90
Manuscript under review for journal Atmos. Meas. Tech.
Discussion started: 5 April 2019

Atmospheric Measurement Techniques Discussions

550 and 700 nm were corrected for truncation errors according to Anderson and Ogren (1998). Absorption coefficients were measured at 470, 532 and 660 nm, and corrected for filter scattering according to Virkkula (2010).

3 Method

The Langley Aerosol Research Group Experiment (LARGE) aircraft team carried out measurements during spiral profiles at altitudes which could range from less than 150m up to greater than 5000m above ground level (ABL) depending on the profile site. On many flight days, these profiles were repeated at each site 3-4 times with individual profiles (ascent or descent) lasting 5 to 15 minutes. AERONET Cimel sun photometers were operated at each ground profile site as well as numerous secondary locations in the vicinity. The profiles used in this study were limited to those where sampling heights covered the majority of the normal aircraft height range to provide an adequately representative column sample. This typical profile depth varied with campaign, e.g. the San Joaquin valley sampling had lower maximum heights due to the prevalent shallow winter boundary layer. Most sun photometer retrievals products (though not volume size distribution) only reach low uncertainty for high aerosol loading ($\geq$ 0.4 at 440nm). Almucantars also must be taken with large solar zenith angle (SZA > 50) and have low residual error (typically < 5%, increasing to a max of 8% at high AOD) for the retrieval calculation to meet Level 2 quality control criteria. Additionally a minimum number of sky radiance measurements in each of four scattering angle bins must meet symmetry requirements in comparison of the two sides (symmetric about the solar azimuth angle) of the almucantar scan. This last criterion effectively requires that the almucantar be taken during cloud-free or minimally cloudy conditions. The LARGE aircraft measurements provided continuous number size distribution data at 1 sec sampling rate for the particle radius range from 0.03 to 0.5 micrometers (in 79 size bins for MD, 25 bins for subsequent campaigns). For comparison with AERONET (fine mode) retrievals, each LARGE in situ sample measurement was converted to aerosol volume size distribution (VSD) and was then weighted by the coincident scattering σ_{SP} at 500nm and averaged for the profile according the following equation.

$$VSD_{(weighted\_mean)} = \frac{\sum_{i=0}^{N} \left[\frac{\sigma_{SP(sample)}}{\sigma_{SP(profile\_mean)}} * VSD_{(sample)}\right]}{N} \qquad \text{N= number of 1 sec samples in profile} \qquad (1)$$

Without such weighting by scattering, the aerosol VSD samples taken within the main aerosol layer would be weighted equally with samples from areas with negligible aerosol where measurement accuracy is diminished. An example of the complete set of individual 1 sec samples from the UHSAS instrument during a full profile can be seen in Figure 2. The flat curves on the bottom of the plot are for the higher altitude samples when aerosol concentrations were very low.

The metrics typically employed to characterize AERONET size distributions are the volume median radius of the fine mode (VMR_f) and the standard deviation or width of the fine mode distribution, sigma, which are standard AERONET inversion products. These parameters were not computed for the LARGE data in this comparison since the upper limit of the UHSAS sampler (0.5 micrometer) is often much less than the calculated fine mode upper boundary of particle radius for the Cimel retrieval algorithm which can vary between 0.439 and 0.992 micrometers, dependent upon the inflection point between fine and coarse modes. Therefore, alternative metrics were used: radius of peak concentration (r_{peak_conc}) and full width half-maximum ($width_{fine\_mode}$) and the size distribution data from the Cimel sun photometer was restricted to the same upper

Atmos. Meas. Tech. Discuss., https://doi.org/10.5194/amt-2019-90
Manuscript under review for journal Atmos. Meas. Tech.
Discussion started: 5 April 2019

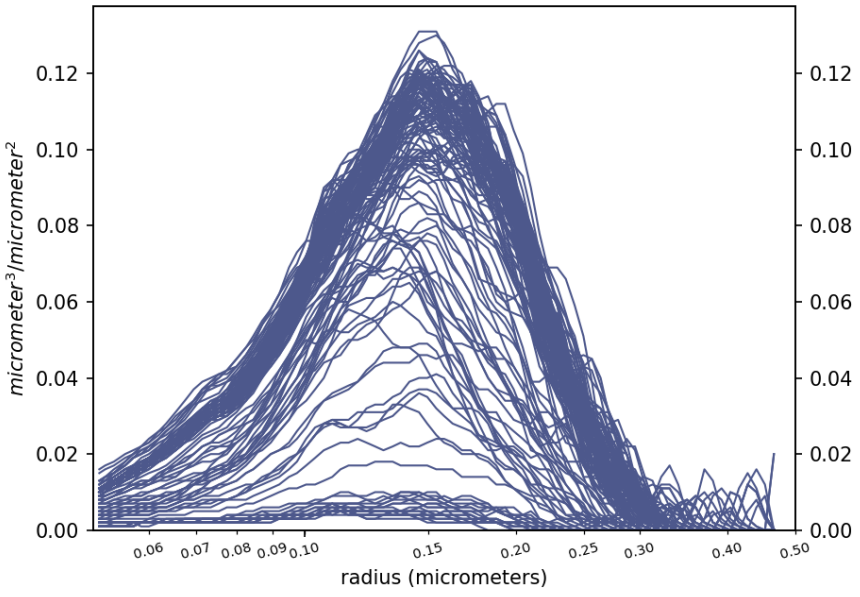

Figure 2. An example of the individual LARGE aerosol 1 sec samples from UHSAS from a full 22 minute aircraft profile at Essex on July 5th, 2011 (11:30 GMT)

radius boundary as the LARGE data for optimal comparability. These alternative metrics were well correlated with our standard retrieval products of VMR_f (r_{peak_conc}: r^2= 0.88) and sigma (distribution width: r^2= 0.63) indicating that they are fair representations of these parameters. Correlation of these metrics with the standard AERONET retrieval products was weaker for larger AOD which would be expected since these conditions would normally be associated with the cases where a larger particle radius upper boundary of the fine mode was determined by the AERONET retrieval. AERONET retrievals acquired within $\pm$ 1 hour of a complete aircraft profile were identified for all four DISCOVER-AQ campaigns in order to compare VSD fine mode metrics derived from AERONET retrievals with those from UHSAS sampling data taken by the LARGE aircraft team.

4 Aerosol Volume Size Distribution Comparisons

AERONET Level 2 (best quality) Version 3 inversions (N=153) derived from AERONET almucantar protocols were matched with concurrently ($\pm$ 1 hour) measured LARGE aircraft profile sampling sequences (N=91). These were compiled to generate statistics for observed AERONET-LARGE average differences (in micrometers, μm) of the computed peak radius of concen-

Atmos. Meas. Tech. Discuss., https://doi.org/10.5194/amt-2019-90
Manuscript under review for journal Atmos. Meas. Tech.
Discussion started: 5 April 2019

Atmospheric Measurement Techniques Discussions

Table 1. Average differences (in μm) in r_{peak_conc} and $width_{fine\_mode}$ between AERONET and LARGE derived values for all campaign comparisons with no humidification adjustments applied. Also, AERONET average r_{peak_conc} and $width_{fine\_mode}$ for each campaign, AERONET-LARGE differences as % of average values and the number of comparisons are shown.

Campaign	$\Delta\ r_{peak\_conc}$	$\Delta\ width_{fine\_mode}$	$\overline{r_{peak\_conc}}$	$\Delta\ peak(\%)$	$\overline{width_{fine\_mode}}$	$\Delta\ width(\%)$	N
MD	0.054±0.027	0.059±0.032	0.233	23.2%	0.211	28.2%	18
CA	0.044±0.039	0.053±0.044	0.189	23.0%	0.170	31.0%	71
TX	0.016±0.020	0.026±0.028	0.148	10.6%	0.127	20.8%	37
CO	0.014±0.020	0.026±0.020	0.143	9.6%	0.123	20.9%	27

tration and VSD fine mode width for the four DISCOVER-AQ campaigns which are presented in Table 1. Here the LARGE measured size distributions are only for dried aerosol data (RH<20%) as compared to retrieved ambient aerosol VSD from AERONET.

Campaign-averaged differences in r_{peak_conc} (AERONET-LARGE) for the four regional campaigns ranged from 0.014μm to 0.054μm micrometers and average volume size distribution width differences ranged from 0.026μm to 0.059μm. Figure 3 depicts color-coded AERONET-derived differences between campaigns. Because AERONET retrievals inherently represent ambient humidity atmospheric conditions, it is to be expected that the size distributions would be shifted to larger sizes for these retrievals relative to LARGE, particularly for more humidified conditions. For the radius of peak concentration there is an increasing trend in AERONET/LARGE differences in the Maryland and Texas data for higher aerosol optical depth which is often correlated with higher relative humidity in these regions due to hygroscopic growth of particle size [Ziemba et al. (2013)]. These campaigns had the most humid conditions and consequently the most frequent occurrence of moderate to high aerosol optical depths. The degree of agreement of VSD fine mode width is not found to be significantly associated with AOD or column water vapor.

Note that the marker size is proportional to the column water vapor acquired by the Cimel sun photometer within $\pm$ 30 minutes of the retrieval. Comparisons for the Colorado campaign show the smallest differences which is consistent with typically small AOD and low relative humidity along the Front Range of the Rocky Mountains. Despite the low to moderate AOD and low column water vapor during the California winter campaign, there are typically larger differences between AERONET and LARGE retrievals of both radius of peak concentration and fine mode width than for the Maryland and Texas comparisons at similar AOD. A possible expanation is that some of these cases are associated with incomplete sampling of the aerosol layer by the aircraft profile for days with particularly shallow boundary layers. The vertical distribution of atmospheric aerosol was quite distinct for the California dataset in that 75% of the aircraft profiles used in these comparisons had the majority of the aerosol below 500m, with 5 profiles where > 90% of aerosol was in this altitude range. The average minimum sampling height in California was 170 meters while the average altitude of peak scattering was only 110 meters higher at 280 meters, so these profiles may be more at risk of missing a moderate portion of the aerosol layer situated below the minimum profile sample altitude. For comparison, the average altitude of maximum aerosol scattering observed by aircraft was $\sim$ 1km in Maryland and $\sim$ 1.2km in Texas and neither of these regions acquired any profiles with such shallow aerosol layers as observed in California.

Atmos. Meas. Tech. Discuss., https://doi.org/10.5194/amt-2019-90
Manuscript under review for journal Atmos. Meas. Tech.
Discussion started: 5 April 2019

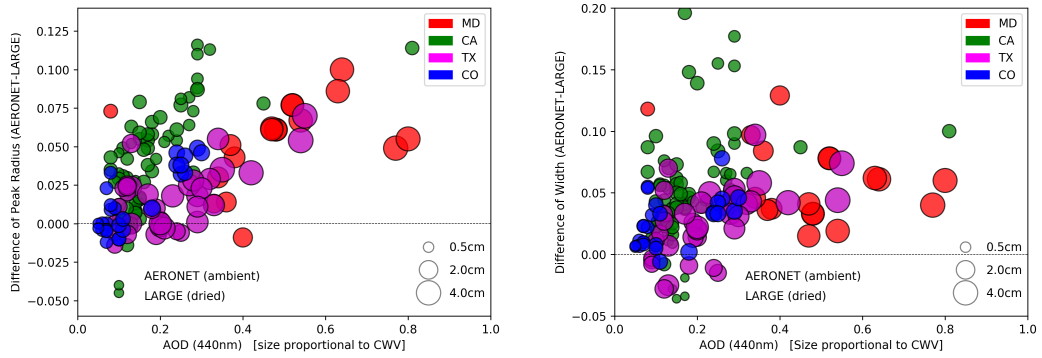

Figure 3. Differences in r_{peak_conc} [left] and $width_{fine\_mode}$ [right] between AERONET (ambient aerosol) and LARGE (dried aerosol) versus AOD (440nm). Marker is size is proportional to coincident column water vapor (CWV in cm) from AERONET

The average fraction of aerosol scattering contributed by the lowest 500m of the atmosphere in Maryland was only 6% (15% for the Texas profiles), whereas in California the lower layer aerosol comprised on average 64% of the total aerosol scattering in the profile. Additionally the California campaign comparisons were also complicated by high frequency of thick morning fog in the San Joaquin Valley during this winter campaign that often generated fog-processed aerosol that changed rapidly in time. It has previously been observed that the influence of persistent fog conditions on aerosol properties can produce significant changes for the hygroscopic fraction and that these changes can also persist beyond the dissipation of the fog or cloud [Eck et al. (2012)]. This type of modification event was documented by Eck et al. (2012) for AERONET inversions of volume size distributions at Fresno, California, a location also included in this DISCOVER-AQ study, where fog-processed aerosols exhibited very large fine radius, even larger than humidified aerosols at high relative humidity and high column water vapor amounts in Maryland and Texas. Both of these factors, typically shallow aerosol layers and frequent and persistent morning fog, could lead to greater potential for disagreement with AERONET measurements for the California campaign. Histograms of the differences in these parameters (for dried aerosol in the LARGE data) are presented for the combined data from all campaign in Figure 4.

4.1 Comparisons With Humidification Adjustment of LARGE Volume Size Distributions

The effect of aerosol humidification on observed differences in the aircraft and AERONET comparisons was estimated using a simple particle growth factor for each UHSAS sample from LARGE. The growth factor depends on the differences between dry and ambient scattering using auxiliary data from on-board nephelometer and Particle Soot Absorption Photometer (PSAP) data. A wavelength independent complex index of refraction was computed from the dry scattering and the dry size distributions and then ambient scattering data was relied on to obtain the ambient refractive index and the growth factors (GF). This size invariant growth factor, scaled by scattering coefficient and averaged for each profile, was used to scale the particle sizes for the dried

Atmos. Meas. Tech. Discuss., https://doi.org/10.5194/amt-2019-90
Manuscript under review for journal Atmos. Meas. Tech.
Discussion started: 5 April 2019

Atmospheric Measurement Techniques Discussions

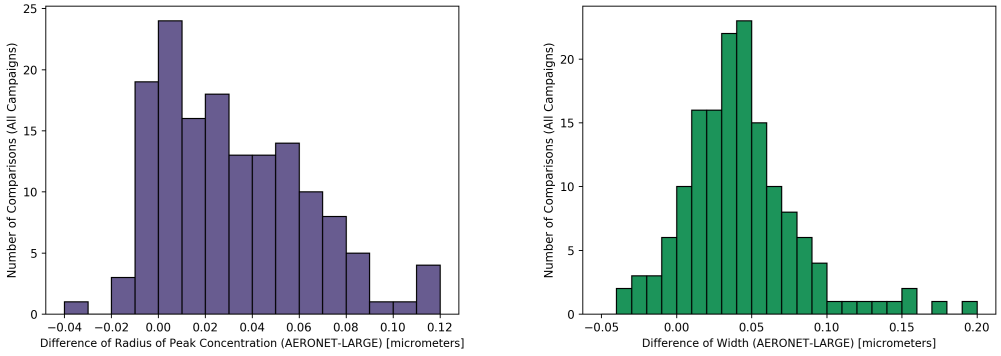

Figure 4. Histograms of all differences of r_{peak_conc} [left] and $width_{fine\_mode}$ [right] between AERONET (ambient aerosol) and LARGE (dried aerosol) for combined campaign comparisons

Table 2. Average differences (in μm) in r_{peak_conc} and $width_{fine\_mode}$ between AERONET and LARGE derived values that include computed humidification adjustments applied to LARGE data. Also, AERONET average r_{peak_conc} and $width_{fine\_mode}$ for each campaign, AERONET-LARGE differences as % of average values and the number of comparisons are shown.

Campaign	$\Delta\ r_{peak\_conc}$	$\Delta\ width_{fine\_mode}$	$\overline{r_{peak\_conc}}$	$\Delta\ peak(\%)$	$\overline{width_{fine\_mode}}$	$\Delta\ width(\%)$	N
MD	0.009±0.015	0.043±0.027	0.191	4.5%	0.184	23.3%	3
CA	0.024±0.016	0.048±0.041	0.183	13.1%	0.173	27.9%	24
TX	0.000±0.015	0.012±0.023	0.148	0.2%	0.124	10.1%	27

aircraft aerosol volume size distribution to better approximate the same columnar ambient VSD as provided by the AERONET retrievals. Not all comparison cases had complete data for all three component sensors (UHSAS, PSAP and nephelometer) so a full profile of growth factor adjusted VSD was not always possible to generate. For the subset of comparisons where the growth factor could be computed, mean differences in VSD statistics were recomputed as shown in Table 2.

The fraction of profiles that had sufficiently complete growth factor computations varied from only 15% of comparisons for Maryland to 57% for Texas. Colorado has no growth factor adjusted cases, though this region would have the least impact from humidification of aerosol due to consistently low RH, as suggested by the relatively good agreement between AERONET retrievals at ambient RH versus LARGE measurements for dried aerosol seen in Table 1. Numerous examples of the VSD from LARGE and AERONET from the three campaigns for cases with computed growth factors are shown in Figure 5.

These depict at least one comparison from 13 sites (on 7 different days) with comparisons where humidification factor could be computed for the LARGE data. The AODs (440nm) associated with this set of comparisons ranged from 0.11 to 0.80 (mean: 0.26). The agreement between concurrent VSDs from AERONET and LARGE is normally improved using the growth factor adjusted data for each of the 3 campaigns for which it could be generated. Note that the agreement of the magnitude of the

Atmos. Meas. Tech. Discuss., https://doi.org/10.5194/amt-2019-90
Manuscript under review for journal Atmos. Meas. Tech.
Discussion started: 5 April 2019

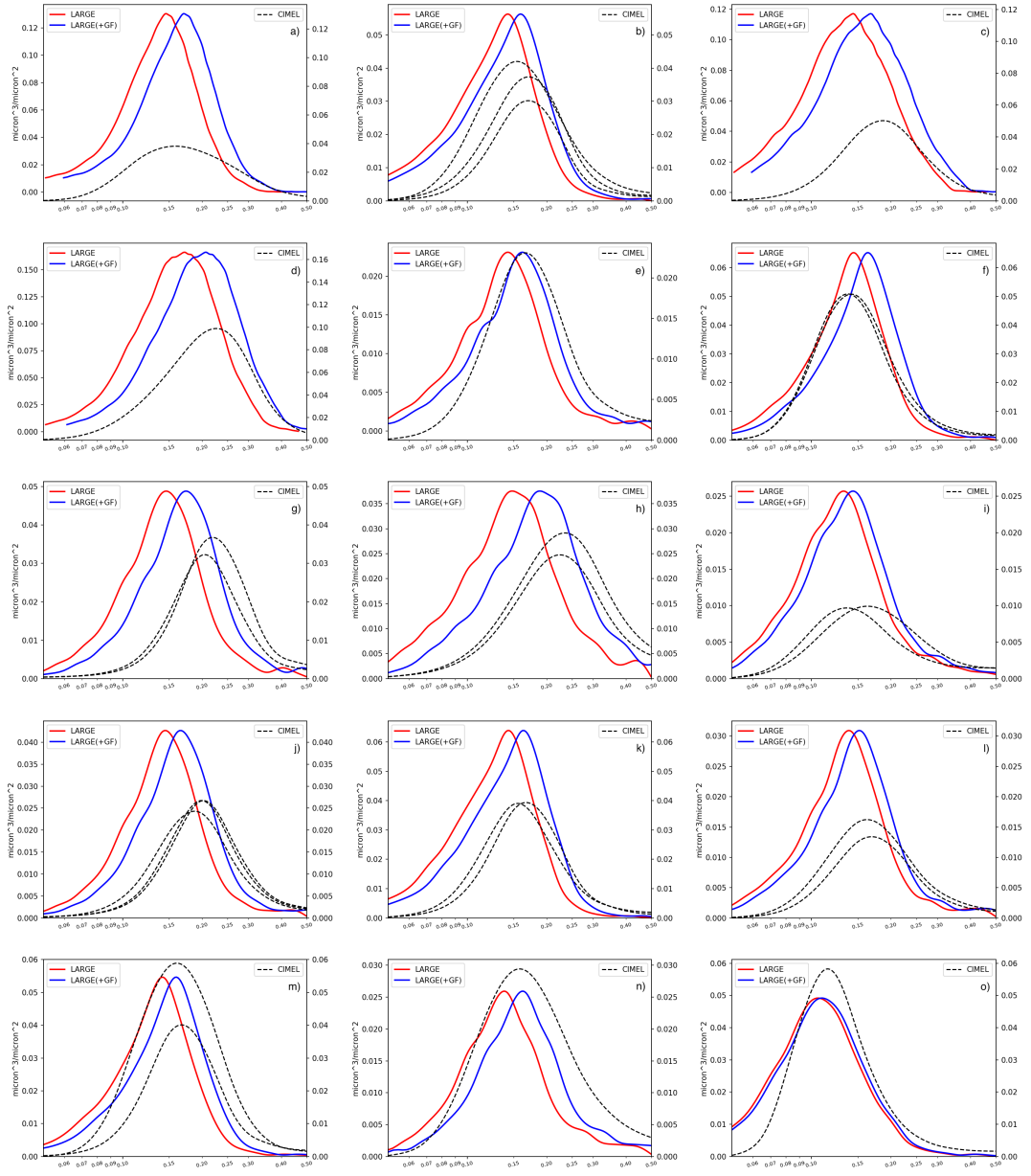

Figure 5. AERONET VSD (dash) comparisons with LARGE (red) and humidified VSD (blue) a) Aldino(MD) [2011-07-05] b) Deer_Park(TX) [2013-09-13] c) Edgewood(MD) [2011-07-05] d) FairHill(MD) [2011-07-29] e) Fresno(CA) [2013-02-01] f) Galveston(TX) [2013-09-13] g) Hanford(CA) [2013-02-01] h) Hanford(CA) [2013-02-04] i) Huron [2013-01-31] j) Huron(CA) [2013-02-01] k) ManvelCroix(TX) [2013-09-13] l) Porterville(CA) [2013-01-31] m) Smith_Point(TX) [2013-09-13] n) Tranquility(CA) [2013-02-01] o) West_Houston(TX) [2013-09-25]

Atmos. Meas. Tech. Discuss., https://doi.org/10.5194/amt-2019-90
Manuscript under review for journal Atmos. Meas. Tech.
Discussion started: 5 April 2019

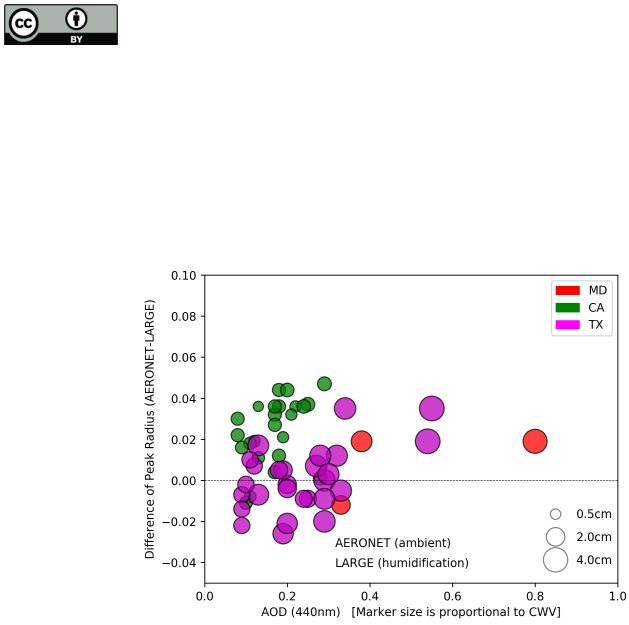

Figure 6. Differences in r_{peak_conc} [left] and $width_{fine\_mode}$ [right] between AERONET (ambient aerosol) and LARGE (with humidification adjustment) versus AOD (440nm) Marker is size is proportional to coincident column water vapor (CWV in cm) from AERONET

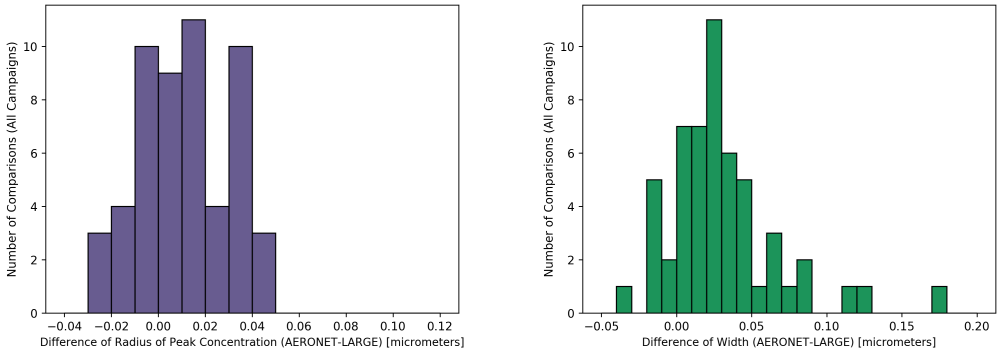

Figure 7. Histograms of all differences of r_{peak_conc} [left] and $width_{fine\_mode}$ [right] between AERONET (ambient aerosol) and LARGE (with humidification adjustment) for combined campaign comparisons

AERONET and LARGE fine mode volume concentration is notably poorer than that for the r_{peak_conc} and $width_{fine\_mode}$ comparisons. This is a result of a known lower sensitivity to this parameter in the sky radiance inversion algorithm. Figure 6 depicts the VSD statistic differences as in Figure 3 but for only the subset of comparisons with humidification adjustment and additionally, the corresponding histograms are seen in Figure 7.

The effect of adding the humidification correction can be directly observed by comparing the difference in VSD metrics for only the subset of cases with corresponding humidified growth factor (GF) adjusted data. For these cases (54 comparisons from 3 campaigns), the combined multi-campaign average of peak radius differences between AERONET and LARGE de-

Atmos. Meas. Tech. Discuss., https://doi.org/10.5194/amt-2019-90
Manuscript under review for journal Atmos. Meas. Tech.
Discussion started: 5 April 2019

Atmospheric Measurement Techniques Discussions

creased from 0.031μm to 0.011μm and the $width_{fine\_mode}$ difference averages decreased from 0.047 μm to 0.031 μm, due to application of humidification growth factors to the LARGE data. The Maryland and Texas campaigns showed the greatest improvement (largest reductions in differences) with very small average differences in peak concentration radius (both < 0.01 μm) when incorporating this simplified humidification assumption. The average difference for the California campaign (N=27) was reduced from 0.043 μm to 0.024μm. As a percentage of the average observed AERONET peak concentration radius this humidification adjusted subset has AERONET-LARGE differences that range from negligible on average for Texas (0.2%) to 9.9% for the California campaign. The best agreement in $width_{fine\_mode}$ parameter was observed for the Texas campaign where the AERONET retrieved width parameter was found to be on average 0.012 μm larger than the humidity adjusted aircraft data which amounts to 10% of the mean value of AERONET VSD width from the AERONET retrievals. The other two campaigns considered here had average $width_{fine\_mode}$ differences that were greater than that noted for Texas (MD: 0.043 μm; CA: 0.044 μm). This may be due in part to the much larger average $width_{fine\_mode}$ of these two campaigns ($\sim$ 0.18 μm) compared with that in Texas (0.12 μm) though the difference as a percent of average campaign $width_{fine\_mode}$ were also larger (23-25%).

The $width_{fine\_mode}$ differences (AERONET-LARGE) decrease for the growth factor adjusted data with campaign averaged differences decreasing for each campaign (Texas: 0.023 μm to 0.012 μm; MD: 0.065 μm to 0.043 μm; California: 0.064 μm to 0.044 μm). For the humidity adjusted dataset, 95% comparisons of the radius of peak concentration agreed within $\pm$ 0.05 μm while 83% of comparisons of the $width_{fine\_mode}$ of the VSD agreed within $\pm$ 0.05 μm. The handful of cases of larger disagreement in $width_{fine\_mode}$ were all from the California campaign which again may reflect incomplete sampling of the full aerosol layer for days with the shallow wintertime boundary layer typical of the region, coupled with potentially extreme growth of fine mode particles in the layer affected by fog in some cases (Eck et al., 2012).

Whereas many AERONET retrieval products such as as imaginary refractive index and single scattering albedo (SSA) require larger AOD (AOD 440 > 0.4) for adequate aerosol absorption signal, it was believed that the volume size distribution did not have similar minimum AOD thresholds for valid determination. However, this had not been empirically verified until this study. With regard to this criterion, the agreement of aircraft and sun photometer was found to have no penalty for conditions of relatively low aerosol loading, at least to the levels measured during these field campaigns. Indeed the mean differences in both peak radius and size distribution width were at a minimum for the lowest AOD cases with smaller standard deviations. For the lowest AOD quartile of the comparison set (AOD 440: 0.09-0.15) the average difference in r_{peak_conc} (AERONET-LARGE) was only 0.011 $\pm$ 0.003 μm compared to the largest quartile (AOD440: 0.27-0.8) average difference of 0.025 $\pm$ 0.008 μm. The low AOD comparisons may benefit in part from the fact that these conditions are more commonly associated with lower relative humidities. As such they might be expected to manifest less disparity between measured (dry) VSD from LARGE and retrieved (ambient) VSD from AERONET especially for hydrophilic aerosol species despite our efforts to approximate and correct for this humidification effect. The corresponding AOD quartile average differences for $width_{fine\_mode}$ were also better for the low AOD comparison set (0.009 $\pm$ 0.003 μm) than the highest quartile (0.019 $\pm$ 0.008 μm). The good agreement in the lowest quartile between aircraft and sun photometer retrievals of both r_{peak_conc} (mean relative differences of 7.8%)

Atmos. Meas. Tech. Discuss., https://doi.org/10.5194/amt-2019-90
Manuscript under review for journal Atmos. Meas. Tech.
Discussion started: 5 April 2019

Atmospheric Measurement Techniques Discussions

and $width_{fine\_mode}$ (7.2%) with small standard deviations strongly suggests that these retrievals are generally stable even at relatively low aerosol optical depths.

5 Conclusions

The DRAGON/DISCOVER-AQ campaigns represent the most extensive comparison of AERONET fine mode column integrated volume size distribution retrievals with in-situ aircraft vertical profile size distribution measurements. These experiments provided a rare opportunity to coordinate multiple instrumented aircraft profiles with AERONET almucantar retrievals at 22 ground sites in Maryland, California, Texas and Colorado during four distinct month-long campaigns (acquired during North American winter, summer and fall seasons) from 2011-2014. Two aerosol fine mode particle size parameters derived from AERONET and LARGE in situ measurement profiles for the four campaigns (radius of peak concentration, r_{peak_conc} and volume size distribution width, $width_{fine\_mode}$) were found to generally agree well for both parameters. The overall average differences (AERONET-LARGE) for r_{peak_conc} was equal to 0.033 $\pm$ 0.035 μm and 0.042 $\pm$ 0.39 μm for $width_{fine\_mode}$. When the aircraft data were adjusted to account for the effect of ambient humidity on the dried aerosol measurements, the results were improved with the combined campaign averaged differences of r_{peak_conc} decreasing significantly to 0.011 $\pm$ 0.019 μm while $width_{fine\_mode}$ average difference decreased to 0.030 $\pm$ 0.039 μm for the subset where humidification adjustments were possible. For this humified subset, the reduced average differences in these parameters represents an improved agreement in AERONET and LARGE comparisons for r_{peak_conc} from an average difference of 15.5% down to 5.2% and a improvement for $width_{fine\_mode}$ from 24.7% to 15.8%. Good agreement was observed over a wide range of aerosol optical depths with comparisons made at AOD (440nm) ranging from 0.09 to 0.8. There were variations in AERONET-LARGE (Cimel-aircraft) mean differences of fine mode metrics between campaigns which were likely a function of differences in average AOD, relative humidity and in the case of the San Joaquin Valley sites, possibly the effect of incomplete sampling of the full aerosol layer when it was particularly shallow.

Acknowledgements. The AERONET project is supported by the Radiation Sciences Program (NASA) and the EOS project office (NASA).
All AERONET data used in this paper are available at "https://aeronet.gsfc.nasa.gov/cgi-bin/webtool_aod_v3" (AOD) and "https://aeronet.gsfc.nasa.gov/cg bin/webtool_inv_v3" (Retrieval products).

References

Anderson, T. L. and Ogren, J. A.: Determining Aerosol Radiative Properties Using the TSI 3563 Integrating Nephelometer, Aerosol Science and Technology, 29, 57–69, https://doi.org/10.1080/02786829808965551, https://doi.org/10.1080/02786829808965551, 1998.

Beyersdorf, A. J., Ziemba, L. D., Chen, G., Corr, C. A., Crawford, J. H., Diskin, G. S., Moore, R. H., Thornhill, K. L., Winstead, E. L., and Anderson, B. E.: The impacts of aerosol loading, composition, and water uptake on aerosol extinction variability in the Baltimore–Washington, D.C. region, Atmospheric Chemistry and Physics, 16, 1003–1015, https://doi.org/10.5194/acp-16-1003-2016, https://www.atmos-chem-phys.net/16/1003/2016/, 2016.

Clarke, A. D., Howell, S., Quinn, P. K., Bates, T. S., Ogren, J. A., Andrews, E., Jefferson, A., Massling, A., Mayol-Bracero, O., Maring, H., Savoie, D., and Cass, G.: INDOEX aerosol: A comparison and summary of chemical, microphysical, and optical properties observed from land, ship, and aircraft, Journal of Geophysical Research: Atmospheres, 107, INX2 32–1–INX2 32–32, https://doi.org/10.1029/2001JD000572, https://doi.org/10.1029/2001JD000572, 2002.

Dubovik, O. and King, M. D.: A flexible inversion algorithm for retrieval of aerosol optical properties from Sun and sky radiance measurements, Journal of Geophysical Research: Atmospheres, 105, 20 673–20 696, https://doi.org/10.1029/2000jd900282, http://dx.doi.org/10.1029/2000JD900282, 2000.

Dubovik, O., Holben, B. N., Lapyonok, T., Sinyuk, A., Mishchenko, M. I., Yang, P., and Slutsker, I.: Non-spherical aerosol retrieval method employing light scattering by spheroids, Geophysical Research Letters, 29, 54–1–54–4, https://doi.org/10.1029/2001gl014506, http://dx.doi.org/10.1029/2001GL014506, 2002.

Dubovik, O., Sinyuk, A., Lapyonok, T., Holben, B. N., Mishchenko, M., Yang, P., Eck, T. F., Volten, H., Muñoz, O., Veihelmann, B., and et al.: Application of spheroid models to account for aerosol particle nonsphericity in remote sensing of desert dust, Journal of Geophysical Research, 111, https://doi.org/10.1029/2005jd006619, http://dx.doi.org/10.1029/2005JD006619, 2006.

Eck, T. F., Holben, B. N., Reid, J. S., Dubovik, O., Smirnov, A., O'Neill, N. T., Slutsker, I., and Kinne, S.: Wavelength dependence of the optical depth of biomass burning, urban, and desert dust aerosols, Journal of Geophysical Research: Atmospheres, 104, 31 333–31 349, https://doi.org/10.1029/1999jd900923, http://dx.doi.org/10.1029/1999JD900923, 1999.

Eck, T. F., Holben, B. N., Sinyuk, A., Pinker, R. T., Goloub, P., Chen, H., Chatenet, B., Li, Z., Singh, R. P., Tripathi, S. N., and et al.: Climatological aspects of the optical properties of fine/coarse mode aerosol mixtures, Journal of Geophysical Research, 115, https://doi.org/10.1029/2010jd014002, http://dx.doi.org/10.1029/2010JD014002, 2010.

Eck, T. F., Holben, B. N., Reid, J. S., Giles, D. M., Rivas, M. A., Singh, R. P., Tripathi, S. N., Bruegge, C. J., Platnick, S., Arnold, G. T., and et al.: Fog- and cloud-induced aerosol modification observed by the Aerosol Robotic Network (AERONET), Journal of Geophysical Research: Atmospheres, 117, n/a–n/a, https://doi.org/10.1029/2011jd016839, http://dx.doi.org/10.1029/2011JD016839, 2012.

Eilenberg, S. R., Bilsback, K. R., Johnson, M., Kodros, J. K., Lipsky, E. M., Naluwagga, A., Fedak, K. M., Benka-Coker, M., Reynolds, B., Peel, J., Clark, M., Shan, M., Sambandam, S., L'Orange, C., Pierce, J. R., Subramanian, R., Volckens, J., and Robinson, A. L.: Field measurements of solid-fuel cookstove emissions from uncontrolled cooking in China, Honduras, Uganda, and India, Atmospheric Environment, 190, 116 – 125, https://doi.org/https://doi.org/10.1016/j.atmosenv.2018.06.041, http://www.sciencedirect.com/science/article/pii/S1352231018304321, 2018.

Feingold, G.: Modeling of the first indirect effect: Analysis of measurement requirements, Geophysical Research Letters, 30, https://doi.org/10.1029/2003gl017967, http://dx.doi.org/10.1029/2003GL017967, 2003.

Gassó, S., Hegg, D. A., Covert, D. S., Collins, D., Noone, K. J., Öström, E., Schmid, B., Russell, P. B., Livingston, J. M., Durkee, P. A., and Jonsson, H.: Influence of humidity on the aerosol scattering coefficient and its effect on the upwelling radiance during ACE-2, Tellus B, 52, 546–567, https://doi.org/10.1034/j.1600-0889.2000.00055.x, https://doi.org/10.1034/j.1600-0889.2000.00055.x, 2000.

Giles, D. M., Sinyuk, A., Sorokin, M. G., Schafer, J. S., Smirnov, A., Slutsker, I., Eck, T. F., Holben, B. N., Lewis, J. R., Campbell, J. R., Welton, E. J., Korkin, S. V., and Lyapustin, A. I.: Advancements in the Aerosol Robotic Network (AERONET) Version 3 database – automated near-real-time quality control algorithm with improved cloud screening for Sun photometer aerosol optical depth (AOD) measurements, Atmospheric Measurement Techniques, 12, 169–209, https://doi.org/10.5194/amt-12-169-2019, https://www.atmos-meas-tech.net/12/169/2019/, 2019.

Gong, S. L., Barrie, L. A., Blanchet, J. P., von Salzen, K., Lohmann, U., Lesins, G., Spacek, L., Zhang, L. M., Girard, E., Lin, H., Leaitch, R., Leighton, H., Chylek, P., and Huang, P.: Canadian Aerosol Module: A size-segregated simulation of atmospheric aerosol processes for climate and air quality models 1. Module development, Journal of Geophysical Research: Atmospheres, 108, AAC 3–1–AAC 3–16, https://doi.org/10.1029/2001JD002002, https://doi.org/10.1029/2001JD002002, 2003.

Holben, B., Eck, T., Slutsker, I., Tanré, D., Buis, J., Setzer, A., Vermote, E., Reagan, J., Kaufman, Y., Nakajima, T., Lavenu, F., Jankowiak, I., and Smirnov, A.: AERONET—A Federated Instrument Network and Data Archive for Aerosol Characterization, Remote Sensing of Environment, 66, 1 – 16, https://doi.org/https://doi.org/10.1016/S0034-4257(98)00031-5, http://www.sciencedirect.com/science/article/pii/S0034425798000315, 1998.

Holben, B. N., Eck, T. F., Slutsker, I., Smirnov, A., Sinyuk, A., Schafer, J., Giles, D., and Dubovik, O.: Aeronet's Version 2.0 quality assurance criteria, Proc. SPIE 6408, Remote Sensing of the Atmosphere and Clouds, 6408, 14 2006.

Li, J., Min, Q., Peng, Y., Sun, Z., and Zhao, J.-Q.: Accounting for dust aerosol size distribution in radiative transfer, Journal of Geophysical Research: Atmospheres, 120, 6537–6550, https://doi.org/10.1002/2015jd023078, http://dx.doi.org/10.1002/2015JD023078, 2015.

Peng, Y., Zhao, J.-Q., Sun, Z., Zhao, W., Wei, X., and Li, J.: Sensitivity of dust radiative forcing to representation of aerosol size distribution in radiative transfer model, Journal of Quantitative Spectroscopy and Radiative Transfer, 219, 292 – 303, https://doi.org/https://doi.org/10.1016/j.jqsrt.2018.04.037, http://www.sciencedirect.com/science/article/pii/S0022407318301122, 2018.

Pueschel, R. F., Russell, P. B., Allen, D. A., Ferry, G. V., Snetsinger, K. G., Livingston, J. M., and Verma, S.: Physical and optical properties of the Pinatubo volcanic aerosol: Aircraft observations with impactors and a Sun-tracking photometer, Journal of Geophysical Research, 99, 12 915, https://doi.org/10.1029/94jd00621, http://dx.doi.org/10.1029/94JD00621, 1994.

Reid, J. S., Koppmann, R., Eck, T. F., and Eleuterio, D. P.: A review of biomass burning emissions part II: intensive physical properties of biomass burning particles, Atmospheric Chemistry and Physics, 5, 799–825, https://doi.org/10.5194/acp-5-799-2005, http://dx.doi.org/10.5194/acp-5-799-2005, 2005.

Sheng, Z., Che, H., Chen, Q., Xia, X., Liu, D., Wang, Z., Zhao, H., Gui, K., Zheng, Y., Sun, T., Li, X., Liu, C., Wang, H., Wang, Y., and Zhang, X.: Aerosol vertical distribution and optical properties of different pollution events in Beijing in autumn 2017, Atmospheric Research, 215, 193–207, https://doi.org/https://doi.org/10.1016/j.atmosres.2018.08.029, http://www.sciencedirect.com/science/article/pii/S0169809518306264, 2019.

Virkkula, A.: Correction of the Calibration of the 3-wavelength Particle Soot Absorption Photometer (3PSAP), Aerosol Science and Technology, 44, 706–712, https://doi.org/10.1080/02786826.2010.482110, https://doi.org/10.1080/02786826.2010.482110, 2010.

Ziemba, L. D., Lee Thornhill, K., Ferrare, R., Barrick, J., Beyersdorf, A. J., Chen, G., Crumeyrolle, S. N., Hair, J., Hostetler, C., Hudgins, C., Obland, M., Rogers, R., Scarino, A. J., Winstead, E. L., and Anderson, B. E.: Airborne observations of aerosol ex-

tinction by in situ and remote-sensing techniques: Evaluation of particle hygroscopicity, Geophysical Research Letters, 40, 417–422, https://doi.org/10.1029/2012GL054428, https://doi.org/10.1029/2012GL054428, 2013.

Atmos. Meas. Tech. Discuss., https://doi.org/10.5194/amt-2019-90
Manuscript under review for journal Atmos. Meas. Tech.
Discussion started: 5 April 2019

Atmospheric Measurement Techniques Discussions

List of Figures

Atmos. Meas. Tech. Discuss., https://doi.org/10.5194/amt-2019-90
Manuscript under review for journal Atmos. Meas. Tech.
Discussion started: 5 April 2019

Atmospheric Measurement Techniques Discussions

List of Tables